

1 **Streamflow elasticity as a function of aridity**

2

3 Vazken Andréassian^{*,1}, Guilherme M. Guimarães¹, Julien Lerat², Alban de Lavenne¹

4

5 ¹ Université Paris-Saclay, INRAE, HYCAR Research Unit, Antony, France

6 ² CSIRO, Canberra, Australia

7 *Corresponding author, vazken.andreassian@inrae.fr

8

9 **Abstract**

10 Relating variations in annual streamflow to a climate anomaly, commonly referred to
11 as *streamflow elasticity to climate*, is central for a rapid assessment of the impact of
12 climate change on water resources. This elasticity is classically estimated via a multiple
13 linear regression between anomalies in streamflow and climate variables. However,
14 this approach does not explicitly account for the fact that elasticity depends on aridity
15 as suggested by “Budyko-type” water balance formulas. Using a large dataset of 4,122
16 catchments from four continents, we first verify empirically the link between elasticity
17 and aridity. Then, we propose a method to constrain elasticity coefficients with
18 derivatives from a “Budyko-type” water balance formula, that allows introducing an
19 explicit dependency between elasticity and aridity. We show that adding this
20 dependency produces a regionalized elasticity formula with physically-realistic
21 elasticity coefficients.

22

23 **Keywords:** elasticity, sensitivity, aridity index, humidity index, Schreiber formula,
24 Oldekop formula, Turc-Mezentsev formula, Bagrov formula, Tixeront-Fu formula,
25 Budyko hypothesis, hierarchical linear model

26 **Notations**

27 This study uses three hydrological fluxes: precipitation (P_n), streamflow (Q_n), and
28 potential evaporation (E_{0n}). All fluxes are computed at the catchment scale as annual
29 sums, expressed in millimeters per year. The subscript n refers to a specific
30 hydrological year. For the Northern Hemisphere, the hydrological year spans from 1st

31 October of year $n - 1$ to 30th September of year n . For the Southern Hemisphere, it
32 spans from 1st April of year n to 31st March of year $n + 1$. Thus, Q_n , represents the
33 streamflow for the hydrological year n . Long-term mean values are denoted by an
34 overbar (e.g., \bar{Q}). Annual anomalies, denoted by Δ , are computed as the difference
35 between the annual value and the long-term mean. For example, the streamflow
36 anomaly is calculated as $\Delta Q_n = Q_n - \bar{Q}$. This is also applied to precipitation ($\Delta P_n = P_n -$
37 \bar{P}) and potential evaporation ($\Delta E_{0n} = E_{0n} - \bar{E}_0$).

38 Additionally, we also define a combined flux, Λ_n (see [Eq. 2Eq-2](#)), which reflects the
39 synchronicity of precipitation and potential evaporation. This is also expressed in
40 millimeters per year, and its anomalies are computed as $\Delta \Lambda_n = \Lambda_n - \bar{\Lambda}$.

41 The *aridity index*, φ , corresponds to the ratio \bar{E}_0/\bar{P} , while the inverse ratio \bar{P}/\bar{E}_0
42 corresponds to the *humidity index*.

43 1 Introduction

44 1.1 About streamflow elasticity

45 The climate elasticity of streamflow (Schaake and Liu, 1989; Dooge et al., 1999;
46 Sankarasubramanian et al., 2001) describes the sensitivity of streamflow to changes
47 in a climate variable. Elasticity is classically derived from the following regression:

$$\Delta Q_n = e_{Q/P} \Delta P_n + e_{Q/E_0} \Delta E_{0n} \quad \text{Eq. 1}$$

48 where: $e_{Q/P}$ denotes the precipitation elasticity of streamflow, e_{Q/E_0} denotes the
49 potential evaporation elasticity of streamflow; both coefficients are dimensionless. Note
50 that elasticity is defined here in absolute terms, i.e. as the sensitivity between quantities
51 of the same dimension (ΔQ , ΔP and ΔE_0 are all in mm/y) following Andréassian et al.
52 (2016).

53 Andréassian et al. (2025) recently proposed to enrich the traditional computation given
54 in [Eq. 1Eq-1](#), to account for the seasonal time shift between precipitation and potential
55 evaporation, because of its decisive impact on catchment water yield (see e.g. Pardé,
56 1933; Coutagne and de Martonne, 1934; Thornthwaite, 1948; Milly, 1994; Yokoo et al.,
57 2008; Roderick and Farquhar, 2011; de Lavenne & Andréassian, 2018; Feng et al.,
58 2019). We compute the synchronous amount of precipitation and potential evaporation
59 Λ , using monthly data as in [Eq. 2Eq-2](#):

$$\Lambda_n = \frac{\sum_{m=1}^{12} \min(P_{m,n}, E_{0,m,n})}{\sqrt{P_n * E_{0n}}} * \bar{P} \quad \text{Eq. 2}$$

60 Where index m stands for the month. The dimension of Λ_n is mm/y and it represents
 61 the annual precipitation volume most easily accessible to evaporation. For two years
 62 with the same annual amounts of precipitation and potential evaporation, Λ will be
 63 higher when they are synchronous, and lower when they are out of phase (for more
 64 details, please refer to Andréassian et al., 2025). With this new term, the regression in
 65 [Eq. 1](#) becomes:

$$\Delta Q_n = e_{Q/P} \Delta P_n + e_{Q/E_0} \Delta E_{0n} + e_{Q/\Lambda} \Delta \Lambda_n \quad \text{Eq. 3}$$

66 1.2 Using aridity to estimate streamflow elasticity

67 The link between streamflow elasticity and catchment aridity is a well-established
 68 concept in hydrology, an idea that can be traced back to Oldekop (1911) and his
 69 followers, including Budyko (1948), Bagrov (1953) and Mezentsev (1955). Many
 70 ‘modern’ hydrologists such as Dooge (1992) and Dooge et al. (1999) discussed the
 71 form that aridity-dependent streamflow formulas could take. This dependency was
 72 emphasized by Koster and Suarez (1999), who write that “*the partitioning of a*
 73 *precipitation anomaly into evaporation and runoff anomalies is a simple function of the*
 74 *dryness index*”, [as well as by Sankarasubramanian et al. \(2001\) who argue that](#)
 75 [empirical elasticity estimates would only follow the direction shown by the Budyko-type](#)
 76 [formulas for the very humid regions of the US](#), while Arora (2002) concludes that “*the*
 77 *use of aridity index provides a straight-forward method to obtain a first order estimate*
 78 *of the effect of climate change on annual runoff*”. Chiew (2006) shows the dependency
 79 of streamflow elasticity on aridity, Renner et al. (2012) stress that the elasticity of
 80 streamflow “*is largely dependent on [...] the aridity of the climate*” and Roderick and
 81 Farquhar (2011) underline that “*the response of runoff to changes in the main driving*
 82 *variables is not constant but depends on the overall climatic dryness*”.

83 More recently, the concept has been applied at a global scale, with Berghuijs et al.
 84 (2017) who use the elasticity pattern provided by the Tixeront-Fu formula to propose a
 85 world map of aridity-dependent streamflow elasticities, Zhang et al. (2022) discuss the
 86 impact of aridity on the sensitivity of the elasticity coefficient to the aggregation time
 87 step, and Anderson et al. (2024) extends the computation of elasticity to different flow

88 quantiles, and show that aridity impacts the shape of the curve relating the different
89 elasticity quantiles.

90 [However, Addor et al. \(2018\), using random forests to explain \(among others\) the](#)
91 [precipitation elasticity of streamflow, concluded that signatures of “hydrological](#)
92 [dynamics are poorly predicted by aridity alone, or even by a combination of several](#)
93 [climatic indices”.](#)

94 **1.3 Local vs class estimation of elasticity**

95 To estimate the climate elasticity of streamflow at regional or national scales, making
96 the dependency of streamflow elasticity on aridity explicit can constrain the estimation
97 of elasticity coefficients and increase their physical realism.

98 For a given catchment with a sufficiently long series of annual observations, streamflow
99 elasticity can be computed *locally* by linear regression (Andréassian et al., 2016).

100 However, for ungauged catchments, local estimation of elasticity coefficients is no
101 longer possible. Instead, a *class*-elasticity can be estimated by combining all available
102 records in a region. The estimation by class has both advantages and drawbacks.
103 While this approach improves the statistical significance of elasticity coefficients, which
104 can have high uncertainty when estimated locally (especially for potential evaporation),
105 it also requires combining data from catchments with different aridity indices. This
106 presents a challenge, precisely because we know that aridity and elasticity are linked.
107 Methods to estimate local- and class-elasticity are detailed in section 2.

108 **1.4 Formulas relating streamflow elasticity to aridity**

109 We mentioned above the seminal work of the hydrologists who, following Oldekop
110 (1911), developed various mathematical formulas to represent catchment water
111 balance. These studies established simple water balance formulas from which a
112 “theoretical” elasticity of streamflow can be derived as their partial derivatives. In [Table](#)
113 [1Table 4](#), we present four long-term water balance formulas that can be used to
114 provide these theoretical elasticity estimates. The Schreiber and Oldekop formulas are
115 parameter-free, while the Turc-Mezentsev and Tixeront-Fu formulas each have one
116 parameter (ω^1 and m , respectively). These last two formulas are equivalent when

¹ We use ω instead of the more commonly used “ n ” on purpose, to avoid confusion with the subscript n used for years.

117 setting $m = \omega + 0.72$ (Yang et al., 2008; Andréassian and Sari, 2018), which explains
118 why their curves overlap in some of the later figures.
119 ~~Table 1~~ [Table 4](#) also presents the partial derivatives for each formula, allowing to
120 compute the precipitation and the potential evaporation elasticities of streamflow.
121 Unsurprisingly, these formulas are all functions of the aridity index.
122

123 Table 1. Common long-term water balance formulas and the associated
 124 elasticities (\bar{Q} – long-term average streamflow [mm/y], \bar{P} – long-term average
 125 precipitation [mm/y], \bar{E}_0 – long-term average reference evaporation [mm/y], $\varphi =$
 126 $\frac{\bar{E}_0}{\bar{P}}$ is the aridity index)

Name	Formula	Precipitation elasticity $\frac{\partial \bar{Q}}{\partial \bar{P}}$	Potential evaporation elasticity $\frac{\partial \bar{Q}}{\partial \bar{E}_0}$
Schreiber (Oldekop, 1911)	$\bar{Q} = \bar{P} \cdot \exp\left(-\frac{\bar{E}_0}{\bar{P}}\right)$ Eq. 4	$e_{Q/P} = (1 + \varphi)e^{-\varphi}$ Eq. 5	$e_{Q/E_0} = -e^{-\varphi}$ Eq. 6
Oldekop (Oldekop, 1911)	$\bar{Q} = \bar{P} - \bar{E}_0 \cdot \tanh\left(\frac{\bar{P}}{\bar{E}_0}\right)$ Eq. 7	$e_{Q/P} = \tanh^2\left(\frac{1}{\varphi}\right)$ Eq. 8	$e_{Q/E_0} = -\tanh\left(\frac{1}{\varphi}\right) + \frac{1}{\varphi} \left[1 - \tanh^2\left(\frac{1}{\varphi}\right)\right]$ Eq. 9
Turc-Mezenisev (Turc, 1954; Mezenisev, 1955)	$\bar{Q} = \bar{P} - [\bar{P}^{-\omega} + \bar{E}_0^{-\omega}]^{\frac{1}{\omega}}$ with $\omega > 0$ Eq. 10	$e_{Q/P} = 1 - (1 + \varphi^{-\omega})^{-\frac{1}{\omega}-1}$ Eq. 11	$e_{Q/E_0} = -(1 + \varphi^\omega)^{-\frac{1}{\omega}-1}$ Eq. 12
Tixeront-Fu (Tixeront, 1964; Fu, 1981)	$\bar{Q} = [\bar{P}^m + \bar{E}_0^{-m}]^{\frac{1}{m}} - \bar{E}_0$ with $m > 1$ Eq. 13	$e_{Q/P} = (1 + \varphi^m)^{\frac{1}{m}-1}$ Eq. 14	$e_{Q/E_0} = -1 + (1 + \varphi^{-m})^{\frac{1}{m}-1}$ Eq. 15

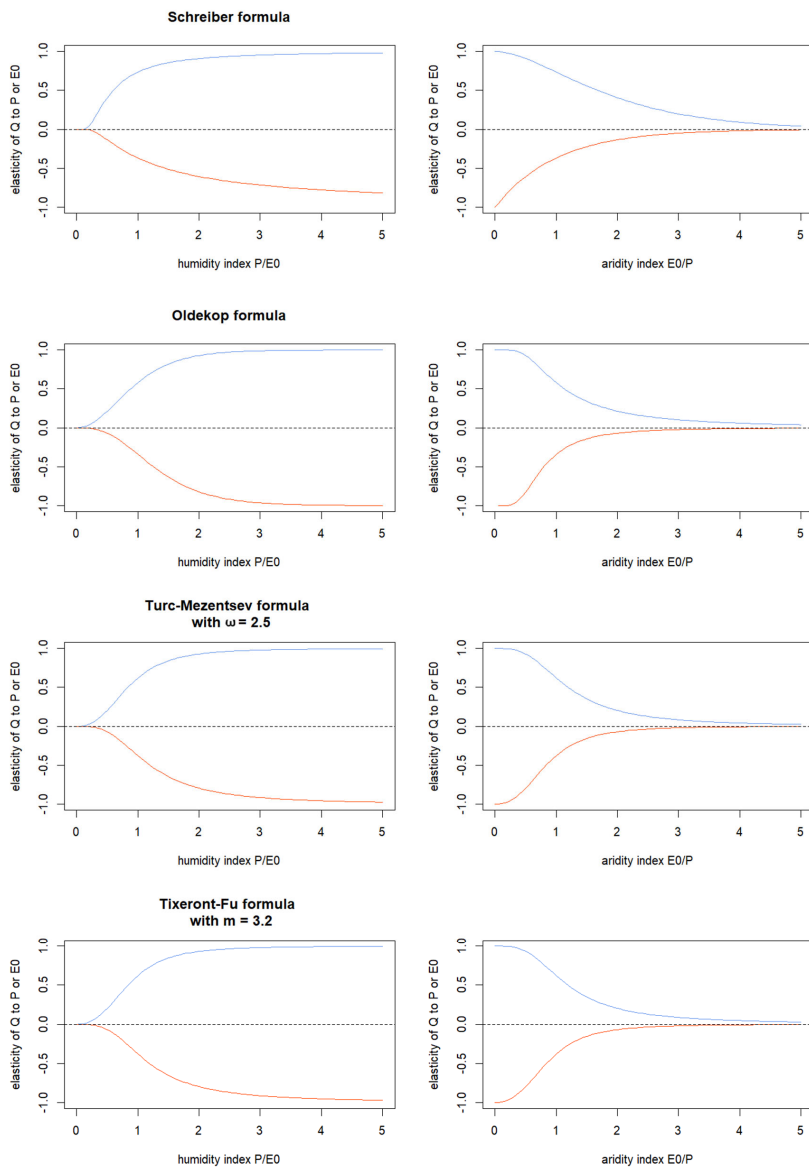
127

128 ~~Figure 1~~ Figure 4 illustrates the similarities and differences among the formulas by
129 showing their respective elasticity-aridity relationships. The embedded dependency on
130 aridity is clearly visible, and we notice that the four formulas have distinct but similar
131 shapes (with the difference between the Turc-Mezentsev and the Tixeront-Fu being
132 negligible). Furthermore, the precipitation elasticity is bounded between 0 and 1, which
133 means that one millimeter of additional precipitation will always result in less than one
134 millimeter of additional streamflow. Similarly, the potential evaporation elasticity is
135 bounded between 0 and -1, which means that one millimeter of additional potential
136 evaporation will always result in a decrease of streamflow of less than one millimeter.
137 These bounds represent a *physically-realistic* catchment response, in the sense that
138 the yield (of the additional mm of precipitation or the additional mm of potential
139 evaporation) must be comprised (in absolute value) between 0 and 100%.

140

141

a mis en forme : Police :Italique



142
 143 **Figure 1: Theoretical relationships between streamflow elasticities and the humidity index (left**
 144 **panel) and the aridity index (right panel). Blue lines represent the precipitation elasticity of**
 145 **streamflow, and orange lines represent the potential evaporation elasticity of streamflow.**

146 1.5 Purpose of this paper

147 This paper aims to verify empirically the fact that streamflow elasticity depends on
148 aridity, and to show how the theoretical pattern provided by the “Budyko-type” water
149 balance formulas can help constrain the estimation of elasticity coefficients, yielding
150 physically-coherent regionalized streamflow elasticities. We use for this purpose a
151 large dataset of catchments covering a wide variety of climates.

152 2 Catchments and Method

153 2.1 Test catchments

154 To ensure that our analysis was based the widest possible range of climates, we used
155 a set of 4,122 catchments, representing 162,005 station-years of data (average length
156 of catchment time series is 39 years). It includes catchments from Australia (Fowler et
157 al., 2024), Brazil (Almagro et al., 2021), Denmark (Liu et al., 2024), France (Delaigue
158 et al., 2024), Germany (Loritz et al., 2024), Sweden (de Lavenne et al., 2022),
159 Switzerland (Höge et al., 2023), the United Kingdom (Coxon et al., 2020) and the USA
160 (Addor et al., 2017). Because this dataset is exactly the same as the one used by
161 Andréassian et al. (2025), we refer the reader to this paper for the details of the
162 selection of the catchments from the original datasets. Let us just mention that we
163 excluded a few catchments with a long memory, for which the linear elasticity model
164 presented in Eq. 16 would not have been justified. Indeed, if a catchment has a
165 hydrogeology that provides it long memory, the elasticity cannot be expressed as a
166 function of the current year climate, but instead should be estimated by accounting for
167 as many previous years as necessary. The absence of interannual memory
168 guarantees the lack of autocorrelation in annual streamflow, which is an important
169 statistical assumption for OLS.

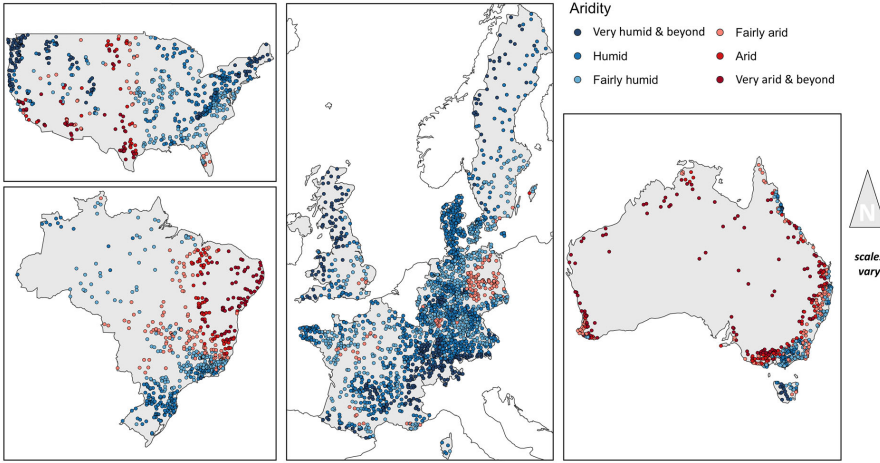
170 In our dataset, the aridity indices range from 0.1 to 6.3, with a first quartile of 0.6 and
171 a third quartile of 1.0. The mean and the median of the aridity index are both 0.8. To
172 assess the generality of the results, we will discuss them at the global scale and also
173 by aridity classes (as defined in Table 2~~Table 2~~).

174

175 Table 2. Aridity classes used in this study (we only kept the classes counting more than 100
 176 catchments)

Aridity class	Average aridity of the class	Number of catchments	Name
[0.25,0.50[0.39	484	Very humid
[0.50,0.75[0.64	1461	Humid
[0.75,1.00[0.85	1238	Fairly humid
[1.00,1.25[1.09	434	Fairly arid
[1.25,1.50[1.37	186	Arid
[1.50,1.75[1.61	109	Very arid

177



178

179 Figure 2. location of the catchments studied and repartition by aridity classes

180

181 2.2 Computation of local elasticities

182 Our reference method will consist in the local (i.e., catchment-specific) computation of
 183 streamflow elasticities using [Eq. 16](#) ~~Eq. 16~~:

$$\Delta Q_n = e_{Q/P}^{loc} \Delta P_n + e_{Q/E_0}^{loc} \Delta E_{0n} + e_{Q/\Lambda}^{loc} \Delta \Lambda_n \quad \text{Eq. 16}$$

184 Because the elasticity coefficients are obtained through linear regression, they are
 185 associated with statistical uncertainty, which we assess using the p-value. A
 186 significance threshold must be chosen, above which a coefficient is not considered
 187 statistically different from zero. For this paper, we use a conventional threshold of 0.05.
 188 With this local approach, a unique triplet of elasticities is computed for each of the
 189 4,122 catchments, and the goodness of fit for each regression is, by definition,
 190 maximized (hence our choice of the local calibration as reference).

191 Note that the correlation between the independent variables of the regression
192 presented in Eq. 16Eq. 16 is rather limited: the correlations computed at the catchment
193 scale are comprised for 90% of the cases in the range [-0.6,0.2] for $(\Delta P_n, \Delta E_{0n})$, in the
194 range [-0.7,0.5] for $(\Delta P_n, \Delta \Lambda_n)$, and in the range [-0.5,0.4] for $\Delta E_{0n}, \Delta \Lambda_n$.

195 2.3 Computation of unique elasticities by aridity class and for the entire dataset

196 We can also estimate a single triplet of elasticities for each different aridity class (as
197 defined in Table 2Table 2) and we then use Eq. 17Eq. 17 for all the catchments of the
198 given aridity class.

$$\Delta Q_n = e_{Q/P}^{cl} \Delta P_n + e_{Q/E_0}^{cl} \Delta E_{0n} + e_{Q/\Lambda}^{cl} \Delta \Lambda_n \quad \text{Eq. 17}$$

199 Estimating a single triplet of elasticities for each class allows investigating the
200 dependency of elasticity to aridity. To calibrate the three parameters, we use a simple
201 grid search algorithm, exploring the following intervals: [-0.1, 1.1] for $e_{Q/P}^{cl}$, and [-1.1, 0.1]
202 for e_{Q/E_0}^{cl} and $e_{Q/\Lambda}^{cl}$, first with a coarse step of 0.1 and then a finer step of 0.01 around
203 the optimum. The objective function to be maximized is the bounded Nash-Sutcliffe
204 Efficiency of Mathevet et al. (2006), which is first calculated for each catchment
205 separately, and then averaged over the catchments belonging to the class and used
206 as the objective to maximize (see Section 2.5).

207 For reference, we also compute a single triplet of elasticities at the global scale by
208 pooling all 4,122 catchments together. By construction, this world-wide triplet yields
209 the lowest mean efficiency.

210 2.4 Computation of regionalized elasticities

211 In the regionalized approach, we use the entire dataset to calibrate a single underlying
212 model, similarly to the calculation of elasticities at the global scale. However, this
213 method ultimately produces catchment-specific results. Each catchment has a distinct
214 triplet of elasticities because the elasticities for precipitation ($e_{Q/P}^{reg}$) and potential
215 evaporation (e_{Q/E_0}^{reg}) are modeled as functions of each catchment's aridity index (φ),
216 given by Eq. 18Eq. 18. The regionalization formulas are adjusted by a shape parameter
217 noted α :

$$\Delta Q_n = e_{Q/P}^{reg} \Delta P_n + e_{Q/E_0}^{reg} \Delta E_{0n} + e_{Q/\Lambda}^{reg} \Delta \Lambda_n \quad \text{Eq. 18}$$

$$e_{Q/P}^{reg} = f_P(\alpha_P, \varphi)$$

$$e_{Q/E_0}^{reg} = f_{E_0}(\alpha_{E_0}, \varphi)$$

$$e_{Q/\Lambda}^{reg} = \text{constant (does not depend on } \varphi)$$

219
 220 There were several alternatives available for choosing the shape of functions f_P , and
 221 f_{E_0} , as well as for adjusting the shape parameters. For f_P and f_{E_0} we used the
 222 derivatives of the Oldekop formula (see [Eq. 8Eq-8](#) and [Eq. 9Eq-9](#)). The variation range
 223 for these functions was constrained based on the results of the class calibration
 224 (Section 2.3). The synchronicity elasticity ($e_{Q/\Lambda}^{reg}$) was kept constant because no clear
 225 empirical relationship was observed when examining either the local or the class-
 226 calibrated elasticities.
 227 [Figure 3Figure 3](#) illustrate the dependency of streamflow elasticities to aridity, which is
 228 apparent both with the locally- and the class-estimated values. To keep the number of
 229 adjusted parameters low, we adjusted only three parameters (α_P , α_{E_0} and $e_{Q/\Lambda}^{reg}$) for [Eq.](#)
 230 [18Eq-18](#), the variation bounds were set up empirically once for all based on the results
 231 of the class calibration.

232 2.5 Model evaluation criterion

233 To evaluate the performance of the different elasticity models in simulating streamflow
 234 anomalies, we use the classical Nash and Sutcliffe (1970) efficiency criterion (NSE).
 235 The NSE is usually computed for each of the 4,122 catchments separately using [Eq.](#)
 236 [19Eq-19](#):

$$NSE = 1 - \frac{\sum_n (\Delta Q_n^{obs} - \Delta Q_n^{cal})^2}{\sum_n (\Delta Q_n^{obs} - \Delta Q_n^{obs})^2} \quad \text{Eq. 19}$$

237 Because the NSE varies in the interval $]-\infty, 1]$, it is not recommended to compute an
 238 average over large sets (indeed, a few very low criteria values will impact the average
 239 criterion value). For this reason, we follow Mathevet et al. (2006) and use the bounded
 240 form (called “C2M” in the original paper) as in [Eq. 20Eq-20](#):

$$\text{Bounded NSE (C2M)} = \frac{NSE}{2 - NSE} \quad \text{Eq. 20}$$

241

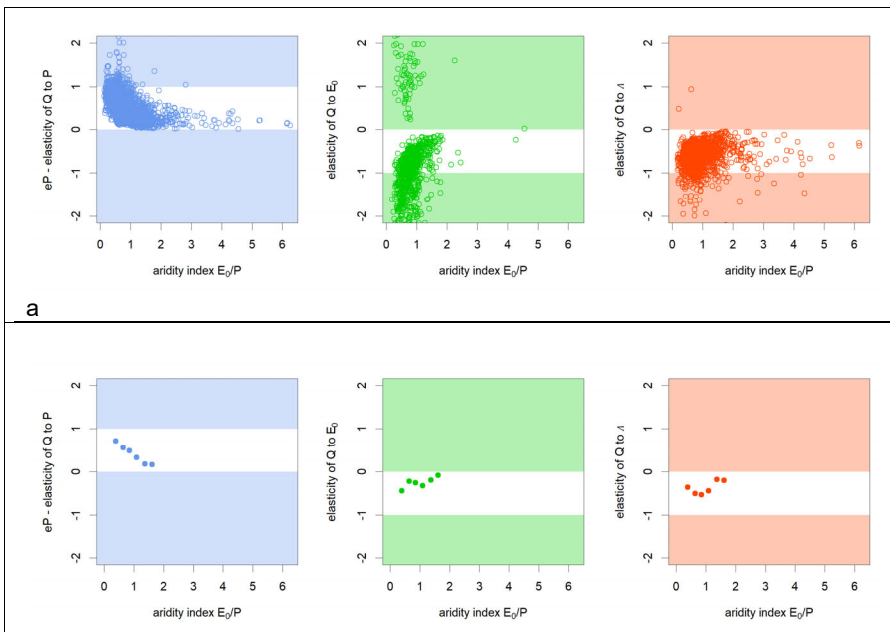
242 **3 Results**

243 **3.1 Empirical verification of the dependency between locally-estimated**
244 **streamflow elasticities and aridity**

245 We first computed the local streamflow elasticities for each catchment by linear
246 regression (Eq. 16), and retained only the coefficients that were statistically
247 significant at the 0.05 level. In our dataset, 97% of the catchments had a significant
248 $e_{Q/P}$ parameter, only 23% of the catchments had a significant e_{Q/E_0} parameter, and
249 64% of the catchments had a significant $e_{Q/\Delta}$ parameter.

250 Figure 3 presents the link between aridity and the locally-estimated elasticity
251 coefficients. The results confirm the expected dependency between precipitation
252 elasticity and aridity, which was previously shown for the theoretical formulas in Figure
253 1. For the potential evaporation elasticity, a satisfying trend is visible but many
254 physically unrealistic elasticities show that additional constraints are required for this
255 term. Finally, the Δ -elasticity of streamflow (i.e. the streamflow elasticity towards the
256 synchronous amounts of precipitation and streamflow), shows no clear dependency
257 on the aridity index (but we did not expect any relationship).

258



b

259 **Figure 3. Relationship between the aridity index and locally-estimated climatic elasticities of**
 260 **streamflow, for precipitation elasticity (left), potential evaporation elasticity (middle),**
 261 **synchronicity elasticity (right). The white domain indicates the physically-plausible range (i.e.**
 262 **[0,1] for precipitation elasticity and [-1,0] for potential evaporation and synchronicity elasticities.**
 263 **a - (upper panel) locally calibrated elasticity coefficients, all plots include only catchments with**
 264 **statistically significant elasticity coefficients ($p < 0.05$), resulting in different sample sizes for**
 265 **each panel ($N = 4017$ for $e_{Q/P}$, $N = 957$ for e_{Q/E_0} and $N = 2630$ for $e_{Q/\Lambda}$); b - (lower panel) class**
 266 **calibrated elasticity coefficients (from Table 3)**
 267

268 3.2 Results by aridity class

269 We also calibrated the three elasticity coefficients to obtain a single triplet of values for
 270 each of the aridity classes as defined in sections 2.4 and 3.2. The resulting class-
 271 calibrated values are presented in Table 3. As reference, the performance of the local
 272 (catchment-specific) estimation is also provided (by construction, it represents the
 273 upper limit of performance).
 274

275 **Table 3. Class-calibrated elasticity values for catchments grouped by the aridity index φ**

Aridity class	Number of catchments	Elasticity values			Performance expressed in mean bounded NSE for	
		$e_{Q/P}^{cl}$	e_{Q/E_0}^{cl}	$e_{Q/\Lambda}^{cl}$	Class approach (same elasticities for all catchments in the same class)	Reference approach (local i.e., catchment-specific estimation)
Very Humid $\varphi \in [0.25, 0.5[$	484	0.72	-0.44	-0.36	0.59	0.68
Humid $\varphi \in [0.5, 0.75[$	1461	0.56	-0.22	-0.50	0.46	0.57
Fairly Humid $\varphi \in [0.75, 1[$	1238	0.49	-0.25	-0.53	0.42	0.52
Fairly Arid $\varphi \in [1, 1.25[$	434	0.33	-0.32	-0.44	0.32	0.49
Arid $\varphi \in [1.25, 1.5[$	186	0.18	-0.19	-0.18	0.27	0.56
Very Arid $\varphi \in [1.5, 1.75[$	109	0.17	-0.08	-0.20	0.29	0.55
World	4,122	0.46	-0.19	-0.56	0.38	0.56

276

277 The numeric values in Table 3 confirm the tendency identified in [Figure 3](#): the
 278 precipitation elasticity of streamflow shows a clear decreasing trend with increasing
 279 aridity, while the potential evaporation elasticity shows a symmetric increasing trend.
 280 The empirical range of variation observed in the class-calibrated results is narrower
 281 than the theoretical range from the water balance formulas: for $e_{Q/P}$, the observed
 282 range is [0.17, 0.72] compared to the theoretical [0, 1], and for e_{Q/E_0} , the range is [-0.44,
 283 -0.08] compared to the theoretical [-1, 0]. Finally, there is no clear trend identifiable for
 284 $e_{Q/A}$. A clear advantage of the class-based calibration approach is that all resulting
 285 elasticities values fall, without exception, within the physically-realistic ranges.

286 3.3 Constraining the elasticity estimation with an aridity-dependent 287 formulation: test for the entire dataset

288 The observed link between the aridity index and the local elasticity estimates
 289 suggested us to test the solution presented in section 2.4, using a “regionalized”
 290 estimation of the elasticities of streamflow. This approach makes use of the identified
 291 pattern to enforce physical coherence across the entire dataset. To parameterize this
 292 relationship, we adapted the partial derivative of the parameter-free Oldekop formula
 293 ([Table 1](#)). We constrained the output of the Oldekop formulas to the empirical
 294 range observed in the class-based calibration (Table 3), offsetting the range for e_p to
 295 [0.15, 0.75], and for e_{E_0} to [-0.45, -0.10]. Thus, the regionalized elasticities are
 296 calculated as:

$$e_{Q/P}^{reg} = 0.15 + |0.75 - 0.15| * f_{P-Oldekop}(\alpha_P, \varphi) \quad \text{Eq. 21}$$

where $f_{P-Oldekop}$ is given by [Eq. 8](#)

$$e_{Q/E_0}^{reg} = -0.10 + |-0.45 + 0.10| * f_{E_0-Oldekop}(\alpha_{E_0}, \varphi) \quad \text{Eq. 22}$$

where $f_{E_0-Oldekop}$ is given by [Eq. 9](#)

298 Note that the restricted ranges remain within the physically-realistic limits.

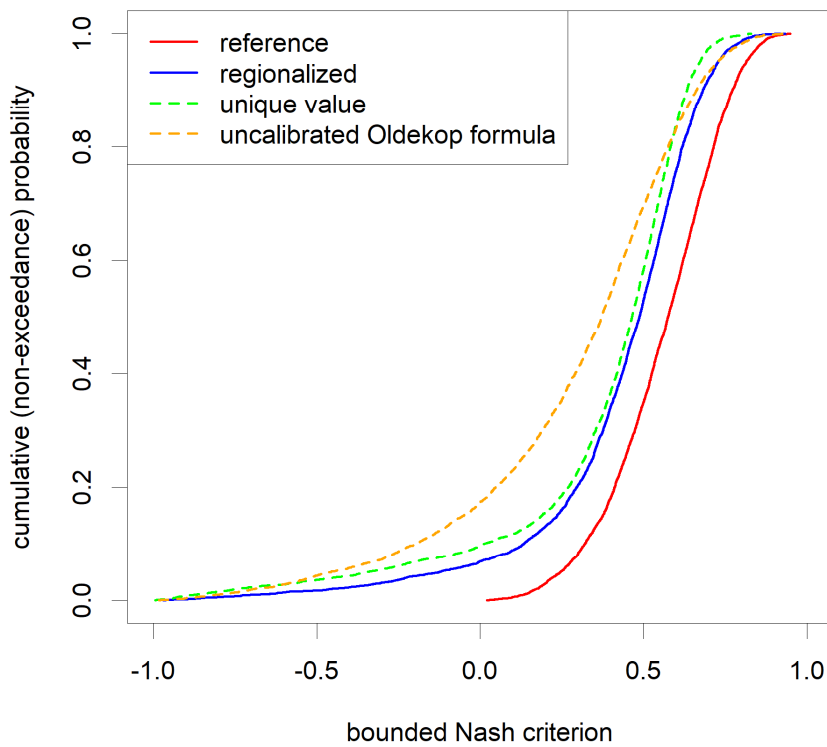
299
 300 We can now compare the performance of three modeling approaches: the “upper
 301 reference” where elasticities are calibrated locally at the catchment scale, the
 302 regionalized approach, and a “lower reference” with elasticities calibrated at global
 303 scale. While the upper reference requires the estimation of 12,366 parameters (3

304 elasticities for 4,122 catchments), the latter two require only 3 parameters each. The
305 corresponding results are presented below in Table 4 and Figure 4.

306
307 **Table 4. Results of the application of the regionalized approach to all the catchments of our**
308 **dataset (4,122): the performance is compared to a upper reference (with locally calibrated**
309 **elasticity values) and a lower reference (with a unique value calibrated for all the catchments in**
310 **the world)**

Performance expressed in mean bounded NSE for		
Upper reference approach: <i>local, i.e. catchment-based estimation</i>	Regionalized approach: <i>elasticities function of each catchment's aridity index</i>	Lower reference approach: <i>same elasticities for all catchments</i>
0.56	0.43	0.38

311
312 There is a clear advantage for taking into account the aridity in the regionalized
313 formula. This approach covers 28% of the performance gap between the lower and
314 upper references, while using only three parameters. In addition, all elasticity
315 parameters remain within the physically-realistic range. The proposed parametrization
316 is therefore successful from both explanatory and predictive point of views, which is a
317 clear advantage (Andréassian, 2023).



318
 319 Figure 4. dDistribution of the performances of the options compared in our paper, with inthe
 320 addition of the uncalibrated theoretical formulation derived from the Oldekop formula. The
 321 (unreachable) upper reference at the extreme right is followed by our regionalized solution,
 322 which has a better performance than an elasticity formula with a unique value (that would be
 323 independent from aridity) or than the elasticities derived from the (uncalibrated) Oldekop
 324 formula.
 325

326 4 Discussion

327 In this paper, our aim was two-fold: (i) to empirically verify that at the catchment scale,
 328 streamflow elasticity and climate aridity are linked, and (ii) to propose an aridity-
 329 dependent parameterization allowing for the quantification of elasticity.

330 4.1 The need for an empirical verification

331 Because of the present popularity of Budyko's framework and its associated theoretical
332 formulas (~~Table 1~~[Table 1](#)), an empirical verification of the elasticity-aridity link might
333 appear superfluous. However, applying these theoretical formulas, such as the
334 Oldekop derivative, relies on a "space-for-time-trade" assumption. This consideration
335 assumes that a model validated across different spatial locations will also be valid for
336 those locations for different time periods (see Peel and Blöschl, 2011, and Singh et al.,
337 2011).

338 Berghuijs and Woods (2016) have warned that this trade requires validation, and
339 Berghuijs et al. (2020) stress that although the Budyko-type curves have been used to
340 predict the evolution of catchments in response to climatic changes, they originate from
341 "*observations of spatial differences in long-term water balances, and not from*
342 *observations or theory of how individual catchments respond to aridity changes*". Thus,
343 we argue that the elasticity-aridity link cannot be taken for granted and requires
344 empirical verification, especially given the mixed results reported by Oudin and
345 Lalonde (2023), [who tested the classical space-time trading when parametrizing a land](#)
346 [use dependent hydrological model, which failed to efficiently predict the direction and](#)
347 [magnitude of hydrological changes after land use conversions.](#)

348 4.2 An aridity-dependent parameterization that uses the shape of the Oldekop 349 formula

350 Regarding our parameterization, our results confirm the general shape of the elasticity-
351 aridity relationship given by the Oldekop formula, but they use a narrower range of
352 variation than the theoretical one. Our work is therefore only partially coherent with the
353 theoretical Budyko-type formulas, which appear to provide a wider range of elasticity
354 values than our empirical data support. This should not be a surprise to hydrologists
355 who know in particular how precipitation intensities impact the hydrological response
356 of arid catchments. What is remarkable, however, is that the intuition of Schreiber
357 (1904) and Oldekop (1911), embedded in formulas of elegant simplicity, remain so
358 useful in the 21st century. We agree on this point with Zhang and Brutsaert (2021) who
359 suggested that the "Budyko hypothesis" could justifiably have been named after
360 Schreiber and Oldekop, who, with so little data and only slide rules, were able to
361 imagine tools still in use today.

Concerning the difference between the elasticities derived from the theoretical Budyko-type formulas and the empirical class-calibrated values, we can suggest two explanations: first, a Budyko-type formula will always remain a conjecture (an elegant, mathematically relevant one, but nevertheless, still a conjecture); second, Gnann et al. (2026) have shown that realistic observational noise will introduce systematic departures from the theoretical optimum.

5 Conclusion

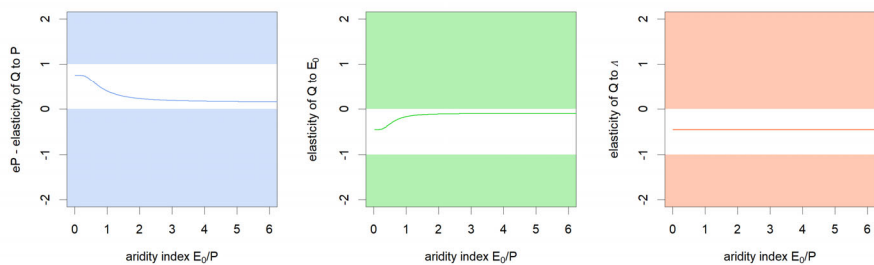
5.1 Summary

In this paper, we investigated the dependency between streamflow elasticity and aridity using a large dataset of 4,122 catchments across Europe, Australia, North America and South America. Our analysis confirmed the well-established dependency between elasticity and aridity and showed that the shape of this dependency can be effectively reproduced by existing theoretical formulas. We further demonstrated that these theoretical formulas can be used to guide the regionalization process, producing a regionalized aridity-dependent estimate of streamflow elasticity for each catchment, based on a parsimonious parameterization. The proposed solution, based on the Oldekop formula, is summarized in Table 5 below and illustrated in Figure 5.

Table 5: Summary of the proposed aridity-accounting regionalized formulas for computing the precipitation and potential evaporation elasticities of streamflow. ΔQ , ΔP , ΔE_0 and $\Delta \Lambda$ are the annual streamflow, precipitation, potential evaporation and synchronicity anomalies, respectively [$mm\ year^{-1}$]. The nondimensional aridity index ($\varphi = \overline{E_0/P}$) is computed as a long-term average. $f_P(\varphi)$ and $f_{E_0}(\varphi)$ are borrowed from the Oldekop formula (see Table 1).

$\Delta Q = e_{Q/P}\Delta P + e_{Q/E_0}\Delta E_0 + e_{Q/\Lambda}\Delta \Lambda$
$e_{Q/P} = 0.15 + 0.6 * f_P(\varphi)$
$f_P(\varphi) = \tanh^2\left(\frac{1}{1.32 * \varphi}\right)$
$e_{Q/E_0} = -0.10 + 0.35 * f_{E_0}(\varphi)$
$f_{E_0}(\varphi) = -\tanh\left(\frac{1}{1.43 * \varphi}\right) + \frac{1}{1.43 * \varphi} \left[1 - \tanh^2\left(\frac{1}{1.43 * \varphi}\right)\right]$
$e_{Q/\Lambda} = -0.47$

a mis en forme : Police :10 pt



386
 387 **Figure 5. Regionalized relationships (from the equations in Table 5-Table 5) for the climatic**
 388 **elasticities of streamflow as a function of the aridity index: precipitation elasticity (left), potential**
 389 **evaporation elasticity (middle), synchronicity elasticity (right). The white domain indicates the**
 390 **physically-plausible range, i.e. [0,1] for precipitation elasticity and [-1,0] for potential evaporation**
 391 **and synchronicity elasticities.**
 392

393 **5.2 Limitations and perspectives**

394 Because our work was empirical, and even if it is based on a very large set of real-
 395 world data, it will remain provisory, until improved by others. It is important to note ~~two~~
 396 three limitations in our study. First, the relationships in Table 5-Table 5 were developed
 397 on catchments with limited interannual memory (in the sense of de Lavenne et al.,
 398 2022): this excludes those catchments for which Eq. 3 would not be warranted to
 399 estimate streamflow elasticity, since additional independent variables expressing the
 400 climatic anomalies of the previous years would have been required. This could have
 401 been done following the work of de Lavenne et al. (2022), or of Pelletier and
 402 Andréassian, (2020), but we preferred to keep the elasticities' estimation as simple as
 403 possible. Second, aridity was computed using the Oudin et al. (2005) formula for
 404 potential evaporation, and the use of other formulas might require a recalibration of the
 405 model parameters. Third, although we do believe that aridity is the first-order driver of
 406 elasticity at the global scale, it is not the only one, and our regional model is clearly
 407 only a first step in the search for physical explanations.
 408

409 **6 Acknowledgements**

410 The authors would like to acknowledge the many individuals that worked to make
411 available the hydrological datasets used in this paper. Special thanks are due to
412 Charles Perrin and Matteo Rosales for their suggestions, [as well as to Manuela](#)
413 [Brunner, Bailey Anderson and Maik Renner for their reviews.](#)

414 **7 Funding**

415 This research has been funded in part by the Agence Nationale de la Recherche
416 (projects CIPRHES ANR-20-CE04-0009 and DRHYM ANR-22-CE56-0007).

417 **8 Author contributions**

418 VA: conceptualization and writing, GMG: computations, figures, discussion, [writing](#)
419 [\(review and editing\)](#), AL: computations, discussion, JL: discussion, writing (review and
420 editing)

421 **9 References**

- 422 [Addor, N., Nearing, G., Prieto, C., Newman, A. J., Le Vine, N., & Clark, M. P.: A](#)
423 [Ranking of Hydrological Signatures Based on Their Predictability in Space. *Water*](#)
424 [Resour Res. 54, 8792–8812, <https://doi.org/10.1029/2018WR022606>, 2018.](#)
- 425 Addor, N., Newman, A.J., Mizukami, N., and Clark, M.P.: The CAMELS data set:
426 catchment attributes and meteorology for large-sample studies, *Hydrol. Earth*
427 *Syst. Sci.*, 21, 5293–5313, <https://dx.doi.org/10.5194/hess-21-5293-2017>, 2017.
- 428 Almagro, A., Oliveira, P.T.S., Alves Meira Neta, A., Roy, T., and Troch, P.: CABra: a
429 novel large-sample dataset for Brazilian catchments, *Hydrol. Earth Syst. Sci.*, 25,
430 3105–3135, <https://doi.org/10.5194/hess-25-3105-2021>, 2021.
- 431 Anderson, B.J., Brunner, M.I., Slater, L.J., and Dadson, S.J.: Elasticity curves describe
432 streamflow sensitivity to precipitation across the entire flow distribution. *Hydrol.*
433 *Earth Syst. Sci.*, 28, 1567–1583, <https://doi.org/10.5194/hess-28-1567-2024>,
434 2024.
- 435 Andréassian, V., Guimarães, G.M., de Lavenne, A., and Lerat, J.: Time shift between
436 precipitation and evaporation has more impact on annual streamflow variability

437 than the elasticity of potential evaporation, *Hydrol. Earth Syst. Sci.*, 29, 5477–
438 5491, <https://doi.org/10.5194/hess-29-5477-2025>, 2025.

439 Andréassian, V.: On the (im)possible validation of hydrogeological models. *C. R.*
440 *Géosci.*, 355 (S1), 337-345, <https://doi.org/10.5802/crgeos.142>, 2023.

441 Andréassian, V. and Sari, T.: Technical Note: On the puzzling similarity of two water
442 balance formulas – Turc-Mezentsev vs Tixeront-Fu. *Hydrol. Earth Syst. Sci.*, 23:
443 2339-2350, <https://dx.doi.org/10.5194/hess-23-2339-2019>, 2019.

444 Andréassian, V., Coron, L., Lerat, J., and le Moine, N.: Climate elasticity of streamflow
445 revisited – an elasticity index based on long-term hydrometeorological records,
446 *Hydrol. Earth Syst. Sci.*, 20, 4503–4524, <https://dx.doi.org/10.5194/hess-20-4503-2016>, 2016.

448 Arora, V.K.: The use of the aridity index to assess climate change effect on annual
449 runoff. *J. Hydrol.*, 265, 164-177, [https://doi.org/10.1016/S0022-1694\(02\)00101-4](https://doi.org/10.1016/S0022-1694(02)00101-4), 2002.

451 Bagrov, N.: On long-term average of evapotranspiration from land surface (О среднем
452 многолетнем испарении с поверхности суши), *Meteorologia i Hidrologia -*
453 *Метеорология и Гидрология*, 10, 20-25, 1953.

454 Berghuijs, W.R., Gnann, S.J., Woods, R.A.: Unanswered questions on the Budyko
455 framework. *Hydrol. Process.*, 34, 5699-5703. <https://doi.org/10.1002/hyp.13958>,
456 2020.

457 Berghuijs, W.R., Larsen, J.R., van Emmerik, T.H.M., and Woods, R.A.: A global
458 assessment of runoff sensitivity to changes in precipitation, potential evaporation,
459 and other factors. *Water Resour. Res.*, 53, 8475–8486.
460 <https://doi.org/10.1002/2017WR021593>, 2017.

461 Berghuijs, W., Woods, R.: Correspondence: Space-time asymmetry undermines water
462 yield assessment. *Nat Commun* 7, 11603,
463 <https://doi.org/10.1038/ncomms11603>, 2016.

464 Budyko, M. I. *Evaporation under natural conditions*, Israel Program for Scientific
465 Translations, Jerusalem, 130 pp., 1948 (1963).

466 Chiew, F.H.S.: Estimation of rainfall elasticity of streamflow in Australia, *Hydrol. Sci.*
467 *J.*, 51, 613–625, <https://doi.org/10.1623/hysj.51.4.613>, 2006.

468 Coutagne, A. and de Martonne, E.: De l'eau qui tombe à l'eau qui coule – évaporation
469 et déficit d'écoulement, *IAHS Red Book series*, 20, 97–128, 1934.

Code de champ modifié

470 Coxon, G., Addor, N., Bloomfield, J. P., Freer, J., Fry, M., Hannaford, J., Howden,
471 N.J.K., Lane, R., Lewis, M., Robinson, E.L., Wagener, T., and Woods, R.:
472 CAMELS-GB: hydrometeorological time series and landscape attributes for 671
473 catchments in Great Britain, *Earth Syst. Sci. Data*, 12, 2459–2483,
474 <https://dx.doi.org/10.5194/essd-12-2459-2020>, 2020.

475 Delaigue, O., Guimarães, G.M., Brigode, P., Génot, B., Perrin, C., Soubeyroux, J.-M.,
476 Janet, B., Addor, N., and Andréassian, V.: CAMELS-FR dataset: a large-sample
477 hydroclimatic dataset for France to explore hydrological diversity and support
478 model benchmarking, *Earth Syst. Sci. Data*, 17, 1461–1479,
479 <https://doi.org/10.5194/essd-17-1461-2025>, 2025.

480 de Lavenne, A., Andréassian, V., Crochemore, L., Lindström, G., and Arheimer, B.:
481 Quantifying pluriannual hydrological memory with Catchment Forgetting Curves,
482 *Hydrol. Earth Syst. Sci.*, 26, 2715–2732, [https://doi.org/10.5194/hess-26-2715-](https://doi.org/10.5194/hess-26-2715-2022)
483 [2022](https://doi.org/10.5194/hess-26-2715-2022), 2022.

484 de Lavenne, A. and Andréassian, V.: Impact of climate seasonality on catchment yield:
485 a parameterization for commonly-used water balance formulas, *J. Hydrol.*, 558,
486 266–274, <https://dx.doi.org/10.1016/j.jhydrol.2018.01.009>, 2018.

487 Dooge, J.C.I.: Sensitivity of runoff to climate change: A Hortonian approach, *Bull. Am.*
488 *Meteorol. Soc.*, 73, 2013–2024, [https://doi.org/10.1175/1520-](https://doi.org/10.1175/1520-0477(1992)073<2013:SORTCC>2.0.CO;2)
489 [0477\(1992\)073<2013:SORTCC>2.0.CO;2](https://doi.org/10.1175/1520-0477(1992)073<2013:SORTCC>2.0.CO;2), 1992.

490 Dooge, J.C., Bruen, M., and Parmentier, B.: A simple model for estimating the
491 sensitivity of runoff to long-term changes in precipitation without a change in
492 vegetation. *Adv Water Resour*, 23, 153–163, [https://doi.org/10.1016/S0309-](https://doi.org/10.1016/S0309-1708(99)00019-6)
493 [1708\(99\)00019-6](https://doi.org/10.1016/S0309-1708(99)00019-6), 1999.

494 Feng, X. Thompson, S.E., Woods, R., and Porporato, I.: Quantifying asynchronicity of
495 precipitation and potential evapotranspiration in Mediterranean climates,
496 *Geophys. Res. Lett.*, <https://doi.org/10.1029/2019GL085653>, 2019.

497 Fowler, K.J.A., Zhang, Z., and Hou, X.: CAMELS-AUS v2: updated
498 hydrometeorological time series and landscape attributes for an enlarged set of
499 catchments in Australia, *Earth Syst. Sci. Data*, 17, 4079–4095,
500 <https://doi.org/10.5194/essd-17-4079-2025>, 2025.

501 Fu, B.: On the calculation of the evaporation from land surface (in Chinese),
502 *Atmospherica Sinica*, 5, 23–31, [https://doi.org/10.3878/j.issn.1006-](https://doi.org/10.3878/j.issn.1006-9895.1981.01.03)
503 [9895.1981.01.03](https://doi.org/10.3878/j.issn.1006-9895.1981.01.03), 1981.

504 [Gnann, S., Anderson, B. J., and Weiler, M.: Uncertainty and non-stationarity of](#)
505 [empirical streamflow sensitivities, EGUsphere \[preprint\],](#)
506 <https://doi.org/10.5194/egusphere-2025-4527>, 2025.

507 Höge, M., Kauzlaric, M., Siber, R., Schönenberger, U., Horton, P., Schwanbeck, J. and
508 Floriancic, M. G. and Viviroli, D. and Wilhelm, S. and Sikorska-Senoner, A.E.,
509 Addor, N., Brunner, M., Pool, S., Zappa, M. and Fenicia, F.: CAMELS-CH: hydro-
510 meteorological time series and landscape attributes for 331 catchments in
511 hydrologic Switzerland, *Earth Syst. Sci. Data*, 15, 5755–5784,
512 <https://doi.org/10.5194/essd-15-5755-2023>, 2023.

513 Koster, R.D., and Suarez, M.J.: A simple framework for examining the interannual
514 variability of land surface moisture fluxes, *J. Clim.*, 12, 1911–1917,
515 [https://doi.org/10.1175/1520-0442\(1999\)012<1911:ASFFET>2.0.CO;2](https://doi.org/10.1175/1520-0442(1999)012<1911:ASFFET>2.0.CO;2), 1999.

516 Loritz, R., Dolich, A., Acuña Espinoza, E., Ebeling, P., Guse, B., Götte, J., Hassler, S.
517 K., Hauffe, C., Heidbüchel, I., Kiesel, J., Mälicke, M., Müller-Thomy, H., Stölzle,
518 M., and Tarasova, L.: CAMELS-DE: hydro-meteorological time series and
519 attributes for 1555 catchments in Germany, *Earth Syst. Sci. Data*, 16, 5625–5642,
520 <https://doi.org/10.5194/essd-16-5625-2024>, 2024.

521 Liu, J., Koch, J., Stisen, S., Trolborg, L., Højberg, A. L., Thodsen, H., Hansen, M. F.
522 T., and Schneider, R. J. M.: CAMELS-DK: hydrometeorological time series and
523 landscape attributes for 3330 Danish catchments with streamflow observations
524 from 304 gauged stations, *Earth Syst. Sci. Data*, 17, 1551–1572,
525 <https://doi.org/10.5194/essd-17-1551-2025>, 2025.

526 Mathevet, T., Michel, C., Andréassian, V. and Perrin, C.: A bounded version of the
527 Nash-Sutcliffe criterion for better model assessment on large sets of basins. *IAHS*
528 *Red Books Series*, 307, 211-219, 2006.

529 Mezentsev, V.: Back to the computation of total evaporation (Ещё раз о расчёте
530 среднего суммарного испарения), *Meteorologia i Hidrologia - Метеорология и*
531 *Гидрология*, 5, 24-26, 1955.

532 Milly, P.C.D.: Climate, interseasonal storage of soil water, and the annual water
533 balance, *Adv. Water Resour.*, 17, 19–24, [https://doi.org/10.1016/0309-](https://doi.org/10.1016/0309-1708(94)90020-5)
534 [1708\(94\)90020-5](https://doi.org/10.1016/0309-1708(94)90020-5), 1994.

535 Nash, J.E. and Sutcliffe, J.V.: River flow forecasting through conceptual models. Part
536 I - a discussion of principles. *J. Hydrol.*, 10, 282-290.
537 [https://doi.org/10.1016/0022-1694\(70\)90255-6](https://doi.org/10.1016/0022-1694(70)90255-6), 1970.

- 538 Oldekor, E.: Evaporation from the surface of river basins (Испарение с поверхности
539 речных бассейнов), Collection of the Works of Students of the Meteorological
540 Observatory, University of Tartu (Jurjew, Dorpat), Tartu, Estonia. [https://ars.els-
541 cdn.com/content/image/1-s2.0-S0022169416300270-mmc1.pdf](https://ars.els-cdn.com/content/image/1-s2.0-S0022169416300270-mmc1.pdf), 1911.
- 542 Oudin, L., Hervieu, F., Michel, C., Perrin, C., Andréassian, V., Anctil, F. and Loumagne,
543 C.: Which potential evapotranspiration input for a rainfall-runoff model? Part 2 –
544 Towards a simple and efficient PE model for rainfall-runoff modelling. *J. Hydrol.*,
545 303: 290-306, <https://dx.doi.org/10.1016/j.jhydrol.2004.08.026> 2005.
- 546 Oudin, L., and Lalonde, M.: Pitfalls of space-time trading when parametrizing a land
547 use dependent hydrological model, *C. R. Géosci.*, 355 (S1): 99-115,
548 <https://doi.org/10.5802/crgeos.146>, 2023.
- 549 Pardé, M.: L'abondance des cours d'eau, *Revue de Géographie Alpine*, 21 (3), 497–
550 542, https://www.persee.fr/doc/rqa_0035-1121_1933_num_21_3_5370, 1933.
- 551 Peel, M. C. and Blöschl, G.: Hydrological modelling in a changing world. *Prog. Phys.*
552 *Geogr.: Earth Environ.*, 35, 249–261, <https://doi.org/10.1177/030913331140255>,
553 2011.
- 554 Renner, M., Seppelt, R., and Bernhofer, C.: Evaluation of water-energy balance
555 frameworks to predict the sensitivity of streamflow to climate change. *Hydrol.*
556 *Earth Syst. Sci.*, 16, 1419–1433, <https://doi.org/10.5194/hess-16-1419-2012>,
557 2012.
- 558 Roderick, M.L., and Farquhar, G.D.: A simple framework for relating variations in runoff
559 to variations in climatic conditions and catchment properties, *Water Resour. Res.*,
560 47, <https://doi.org/10.1029/2010WR009826>, 2011.
- 561 Sankarasubramanian, A., Vogel, R.M., and Limbrunner, J.F.: Climate elasticity of
562 streamflow in the United States, *Water Resour. Res.*, 37, 1771–1781,
563 <https://doi.org/10.1029/2000wr900330>, 2001.
- 564 Schaake, J., and Liu, C.: Development and application of simple water balance models
565 to understand the relationship between climate and water resources, *New*
566 *Directions for Surface Water Modeling*, IAHS Red Book series n°181, 343–352,
567 <https://iahs.info/uploads/dms/7849.343-352-181-Schaake-Jr.pdf>, 1989.
- 568 Schreiber, P.: On the relationship between precipitation and river flow in central Europe
569 (Über die Beziehungen zwischen dem Niederschlag und der Wasserführung der
570 Flüsse in Mitteleuropa). *Zeitschrift für Meteorologie*, 21, 441–452, 1904.

Code de champ modifié

571 Singh, R., Wagener, T., van Werkhoven, K., Mann, M. E., and Crane, R.: A trading-
572 space-for-time approach to probabilistic continuous streamflow predictions in a
573 changing climate – accounting for changing watershed behavior, *Hydrol. Earth*
574 *Syst. Sci.*, 15, 3591–3603, <https://doi.org/10.5194/hess-15-3591-2011>, 2011.

575 Thornthwaite, C.W.: An approach toward a rational classification of climate. *Geog.*
576 *Rev.*, 38 (1), 55–94. <https://doi.org/10.2307/210739>, 1948.

577 Tixeront, J.: Prediction of streamflow (in French: Pr evision des apports des cours
578 d'eau). IAHS publication, 63, 118-126, 1964.

579 Turc, L.: The water balance of soils: relationship between precipitations, evaporation
580 and flow (In French: Le bilan d'eau des sols: relation entre les pr ecipitations,
581 l' vaporation et l' coulement), *Annales Agronomiques, S rie A*, 5, 491-595,
582 1954.

583 Yang, H., Yang, D., Lei, Z., and Sun, F.: New analytical derivation of the mean annual
584 water-energy balance equation, *Water Resour. Res.*, 44, W03410,
585 <https://doi.org/03410.01029/02007WR006135>, 2008.

586 Yokoo, Y., Sivapalan, M., and Oki, T.: Investigating the role of climate seasonality and
587 landscape characteristics on mean annual and monthly water balances, *J.*
588 *Hydrol.*, 357, 255–269, <https://doi.org/10.1016/j.jhydrol.2008.05.010>, 2008.

589 Zhang, L., and Brutsaert, W: Blending the evaporation precipitation ratio with the
590 complementary principle function for the prediction of evaporation. *Water Resour.*
591 *Res.*, 57, e2021WR029729. <https://doi.org/10.1029/2021WR029729>, 2021.

592 Zhang, Y., Viglione, A., and Bl oschl, G.: Temporal scaling of streamflow elasticity to
593 precipitation: A global analysis. *Water Resour. Res.*, 58, e2021WR030601.
594 <https://doi.org/10.1029/2021WR030601>, 2022.

595

a mis en forme : Franais (France)

a mis en forme : Franais (France)